

# Experimental validation of an analytical model for nonlinear propagation in uncompensated optical links

E. Torrenco,<sup>1</sup> R. Cigliutti,<sup>1</sup> G. Bosco,<sup>1</sup> A. Carena,<sup>1,\*</sup> V. Curri,<sup>1</sup> P. Poggiolini,<sup>1</sup>  
A. Nespola,<sup>2</sup> D. Zeolla,<sup>2</sup> and F. Forghieri<sup>3</sup>

<sup>1</sup>*OptCom, Dipartimento di Elettronica, Politecnico di Torino, Corso Duca degli Abruzzi, 24, 10129, Torino, Italy*

<sup>2</sup>*Istituto Superiore Mario Boella, Via Pier Carlo Boggio 61, 10131, Torino, Italy*

<sup>3</sup>*CISCO Photonics, Via Philips 12, 20059, Monza, Italy*

\*[andrea.carena@polito.it](mailto:andrea.carena@polito.it)

**Abstract:** Link design for optical communication systems requires accurate modeling of nonlinear propagation in fibers. This topic has been widely analyzed in last decades with partial successes in special conditions, but without a comprehensive solution. Since the introduction of coherent detection with electronic signal processing the scenario completely changed because this category of systems shows better performances in links without in-line dispersion management. This change to uncompensated transmission allowed to modify the approach in the study of nonlinear fiber propagation and in recent years a series of promising analytical models have been proposed. In this paper, we present an experimental validation over different fiber types of an analytical model for nonlinear propagation over uncompensated optical transmission links. Considering an ultra-dense WDM system, we transmitted ten 120-Gb/s PM-QPSK signals over a multi-span system probing different fiber types: SSMF, PSCF and NZDSF. A good matching was found in all cases showing the potential of the analytical model for accurate performance estimation that could lead to powerful tools for link design.

©2011 Optical Society of America

**OCIS codes:** (060.1660) Coherent communications; (060.2330) Fiber optics communications.

---

## References and links

1. G. Agrawal, *Nonlinear Fiber Optics* (Academic, San Diego, 2007).
2. D. Marcuse, C. R. Manyuk, and P. K. A. Wai, "Application of the Manakov-PMD equation to studies of signal propagation in optical fibers with randomly varying birefringence," *J. Lightwave Technol.* **15**(9), 1735–1746 (1997).
3. V. Curri, P. Poggiolini, A. Carena, and F. Forghieri, "Dispersion compensation and mitigation of nonlinear effects in 111-Gb/s WDM coherent PM-QPSK systems," *IEEE Photon. Technol. Lett.* **20**(17), 1473–1475 (2008).
4. M. S. Alfiad, D. van den Borne, T. Wuth, M. Kuschnerov, and H. de Waardt, "On the tolerance of 111-Gb/s POLMUX-RZ-DQPSK to nonlinear transmission effects," *J. Lightwave Technol.* **29**(2), 162–170 (2011).
5. P. Poggiolini, A. Carena, V. Curri, G. Bosco, and F. Forghieri, "Analytical modeling of non-linear propagation in uncompensated optical transmission links," *IEEE Photon. Technol. Lett.* **23**(11), 742–744 (2011).
6. M. Nazarathy, J. Khurgin, R. Weidenfeld, Y. Meiman, P. Cho, R. Noe, I. Shpantzer, and V. Karagodsky, "Phased-array cancellation of nonlinear FWM in coherent OFDM dispersive multi-span links," *Opt. Express* **16**(20), 15777–15810 (2008).
7. B. Goebel, B. Fesl, L. D. Coelho, and N. Hanik, "On the effect of FWM in coherent optical OFDM systems," in *Optical Fiber Communication Conference and Exposition and The National Fiber Optic Engineers Conference*, OSA Technical Digest (CD) (Optical Society of America, 2008), paper JWA58.
8. X. Chen and W. Shieh, "Closed-form expressions for nonlinear transmission performance of densely spaced coherent optical OFDM systems," *Opt. Express* **18**(18), 19039–19054 (2010).
9. H. Louchet, A. Hodzic, and K. Petermann, "Analytical model for the performance evaluation of DWDM transmission systems," *IEEE Photon. Technol. Lett.* **15**(9), 1219–1221 (2003).
10. J. Tang, "A comparison study of the Shannon channel capacity of various nonlinear optical fibers," *J. Lightwave Technol.* **24**(5), 2070–2075 (2006).

11. P. Poggiolini, G. Bosco, A. Carena, V. Curri, and F. Forghieri, "A simple and accurate model for non-linear propagation effects in uncompensated coherent transmission links," in *2011 13th International Conference on Transparent Optical Networks (ICTON)* (2011), paper We.B1.3.
  12. A. Carena, V. Curri, G. Bosco, P. Poggiolini, and F. Forghieri, "Modeling of the impact of non-linear propagation effects in uncompensated optical coherent transmission links," *J. Lightwave Technol.* (submitted to).
  13. E. Torrenco, R. Cigliutti, G. Bosco, A. Carena, V. Curri, P. Poggiolini, A. Nespola, D. Zeolla, and F. Forghieri, "Experimental validation of an analytical model for nonlinear propagation in uncompensated optical links," in *37th European Conference and Exposition on Optical Communications*, OSA Technical Digest (CD) (Optical Society of America, 2011), paper We.7.B.2.
  14. G. Bosco, A. Carena, R. Cigliutti, V. Curri, P. Poggiolini, and F. Forghieri, "Performance prediction for WDM PM-QPSK transmission over uncompensated links," in *Optical Fiber Communication Conference*, OSA Technical Digest (CD) (Optical Society of America, 2011), paper OThO7.
  15. E. Grellier and A. Bononi, "Quality parameter for coherent transmissions with Gaussian-distributed nonlinear noise," *Opt. Express* **19**(13), 12781–12788 (2011).
  16. S. Benedetto and E. Biglieri, *Principles of Digital Transmission: with Wireless Applications* (Kluwer, New York, 1999).
  17. G. Bosco, R. Cigliutti, E. Torrenco, A. Carena, V. Curri, P. Poggiolini, and F. Forghieri, "Joint DGD, PDL and chromatic dispersion estimation in ultra-long-haul WDM transmission experiments with coherent receivers," in *2010 36th European Conference and Exhibition on Optical Communication (ECOC)* (2010), paper Th.10.A.2.
- 

## 1. Introduction

Nonlinear propagation in optical fibers has been extensively studied –over the last two decades to support link design with the understanding of the physical behavior of signal propagation. A proven analytical model is based on the well-known non-linear Schrödinger equation [1] and on the Manakov extension [2] when polarization effects must also be taken into account. Both these models have been largely validated during past years but they lack a closed-form solution and their use requires numerical simulations which are very time-consuming. To speed up link design and validation processes, a search for simplified and approximate models with compact solutions has been carried out by researchers. The analysis of dispersion managed links and intensity modulation systems led to partial successes, limited to specific cases and effects. The introduction of coherent detection with electronic signal processing at the receiver completely changed the scenario of operation: uncompensated transmission (UT) has been shown to be preferable with respect to dispersion management because of increased performances [3,4]. Under this condition, the study of nonlinear propagation starts with new and different hypotheses.

Recently, various analytical models for UT links have been proposed, such as [5–10]. A common baseline for all of them is a perturbative approach assuming nonlinear effects are mild in the regime of interest. We can group these models in two categories: some are based on a frequency-discrete approach [5–8], while others on truncated Volterra-series [9,10]. Most of them bear substantial similarities in their assumptions and analytical results. In this paper, we concentrate on [5], whose very good accuracy in performance prediction has been extensively validated through simulations both for polarization-multiplexed quadrature phase-shift keying (PM-QPSK) at the Nyquist limit [5] (i.e., at baud-rate channel spacing with rectangular spectra) and at wider channel spacings with various PM-QAM (quadrature-amplitude modulation) formats with higher cardinality [11,12].

In this work we extend the set of results presented in [13] providing a broad experimental validation of this analytical model: we compare model predictions with measurements carried out in a wavelength-division multiplexing (WDM) experiment with ten 30-Gbaud PM-QPSK channels, spaced 33 GHz. We tested the transmission over a multi-span optical link and we probed three different fiber types in order to assess the validity of the model with substantially different loss, dispersion and non-linearity parameters. In order to successfully reach the goal of validating the nonlinear propagation model, all parameters in our experiment have been carefully measured and a back-to-back calibration was required. In the end, a good matching was found in all three analyzed cases, suggesting that the analytical model is accurate enough to be used as an efficient tool for performance estimation in long-haul experiments over uncompensated fiber links.

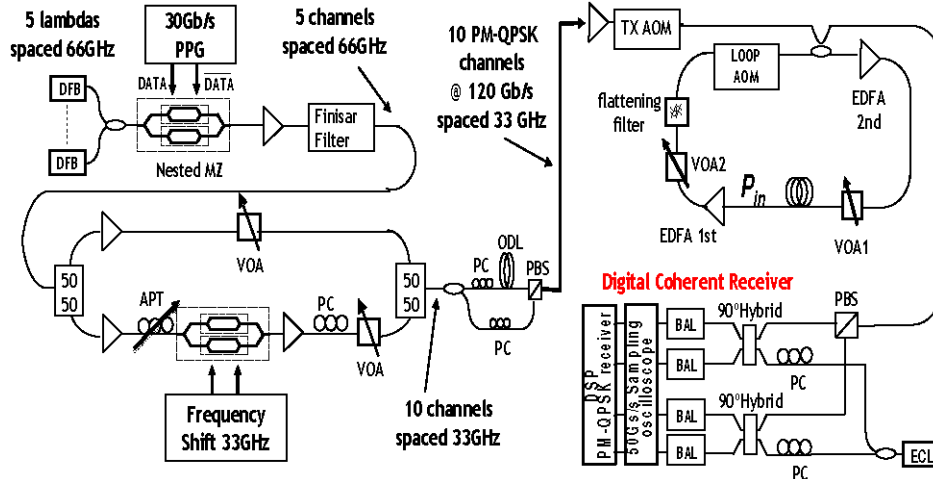


Fig. 1. Experimental set-up for the generation and transmission of ten 120 Gb/s PM-QPSK signals with 33 GHz spacing.

This paper is structured as follows: in Sect. 2 we introduce the experimental setup used for measurements based on a recirculating loop, where we propagated a set of ten 120 Gbps PM-QPSK Nyquist-WDM channels over different fiber types. In Sect. 3 we explain how to calibrate out the effect of inter-channel crosstalk and all other transmitter and receiver impairments based on back-to-back measurements. In Sect. 4 we introduce transmission results and we show the agreement with model prediction in different conditions. Finally, we draw some conclusions.

## 2. Experimental setup

The experimental setup is shown in Fig. 1. Five Distributed Feedback (DFB) lasers were used to generate continuous wave (CW) frequencies spaced 66 GHz. Then a 30-Gbaud QPSK modulation was applied to these carriers using a Nested Mach-Zehnder (NMZ) modulator. This 5-channel WDM signal was then narrow-filtered using a reconfigurable Finisar optical Waveshaper filter, with  $-3$  dB bandwidth equal to 32 GHz: this unit is capable of generating all pass-bands at once. Such tight filtering shapes channels spectra and it is needed to limit crosstalk in the Nyquist-WDM scenario where we carried out our measurements. All five 66-GHz-spaced QPSK channels were then launched into an optical frequency-doubler, made of a pass-through branch and a frequency-shifter (FS) branch. The latter includes a NMZ modulator operated as a FS, configured to shift the five input channels by 33 GHz. The pass-through and FS branches were delayed for decorrelation and then combined to form a 10-channel, 33-GHz spaced QPSK signal comb. This signal was sent to a polarization-multiplexing stage to form a 10-channel WDM PM-QPSK signal with 33 GHz spacing, whose power spectrum is shown in Fig. 2(a). Each PM-QPSK channel carries 120 Gb/s.

The WDM signals were then launched into a re-circulating fiber loop, including a dual-stage Erbium-Doped Fiber Amplifier (EDFA) which completely recovered the span losses. Three different types of fiber were used: a standard single-mode fiber (SSMF), a pure silica-core fiber (PSCF) and a non-zero dispersion shifted fiber (NZDSF). All fiber parameters (span length  $L_s$ , loss coefficient  $\alpha$ , total span loss  $A_{span}$ , dispersion  $D$ , nonlinearity coefficient  $\gamma$ ) are reported in Table 1. The value of  $A_{span}$  includes the actual fiber loss plus all other extra-losses present between the input of the fiber and the input of the EDFA 1st stage. A variable optical attenuator (VOA), labeled VOA1 in Fig. 1, was used to change the  $P_{Tx, ch}$  at the input of the fiber under test. A gain-flattening filter, the loop acousto-optic switch and the 3dB coupler were inserted between the EDFA stages.

**Table 1. Parameters of the fibers used in the experiments**

	$L_s$ [km]	$\alpha$ [dB/km]	$A_{span}$ [dB]	$D$ [ps/nm/km]	$\gamma$ [ $W^{-1}km^{-1}$ ]
SSMF	102	0.21	22.5	16.75	1.26
PSCF	98	0.18	19.6	20.6	1.0
NZDSF	100	0.22	23.5	2.58	2.0

The dual-stage EDFA equivalent noise figure  $F_{eq}$  was accurately characterized as a function of the power level  $P_{in}$  entering the 1st stage of the amplifier. The values of  $F_{eq}$  as a function of  $P_{in}$  are shown in Fig. 2(b) and have been used in the analytical performance prediction to properly account for amplified spontaneous emission (ASE) noise accumulation in the experiment. Noise loading was not present in the setup: the only source of ASE noise was the dual-stage EDFA in the loop. The receiver (Rx) had a standard set-up for coherent reception and used linear-amplified dual-balanced photodetectors with 30 GHz bandwidth. Channel selection was performed exclusively by tuning the local oscillator (LO). The four photodetectors electrical signals were digitized at 50 GSamples/s using a Tektronix DPO71604 real-time scope with  $-3$  dB electrical bandwidth equal to 16 GHz. The sampling rate was 1.66 samples/symbol. The Rx digital signal processing (DSP) consisted of a CD-compensation first stage followed by a 25-taps multiple-input multiple-output (MIMO) stage adjusted through a decision-driven constant modulus algorithm (CMA), followed in turn by frequency estimation and a Viterbi&Viterbi stage. Measurements of bit-error-rate (BER) were carried out on the center wavelength in the WDM comb using both for the channel and for the local oscillator (LO) two distinct external-cavity lasers (ECL), each with a linewidth of about 100 kHz.

### 3. Back-to-back measurements and calibration

According to [14,15], the performance of an optical link can be estimated using a generalized optical signal-to-noise ratio (OSNR), defined as:

$$OSNR_{NL} = \frac{P_{Tx,ch}}{P_{ASE} + P_{NLI}} \quad (1)$$

where  $P_{Tx,ch}$  is the power per channel launched into the fiber,  $P_{ASE} = N_s F (A_{span} - 1) h \nu B_n$  is the ASE noise power,  $N_s$  is the number of spans,  $F$  is the amplifier noise figure,  $h$  is Plank's constant,  $\nu$  is the center frequency of the center channel and  $B_n$  is the noise reference bandwidth. In the following  $B_n$  is always set to 0.1 nm.  $P_{NLI}$  is the power of the non-linear

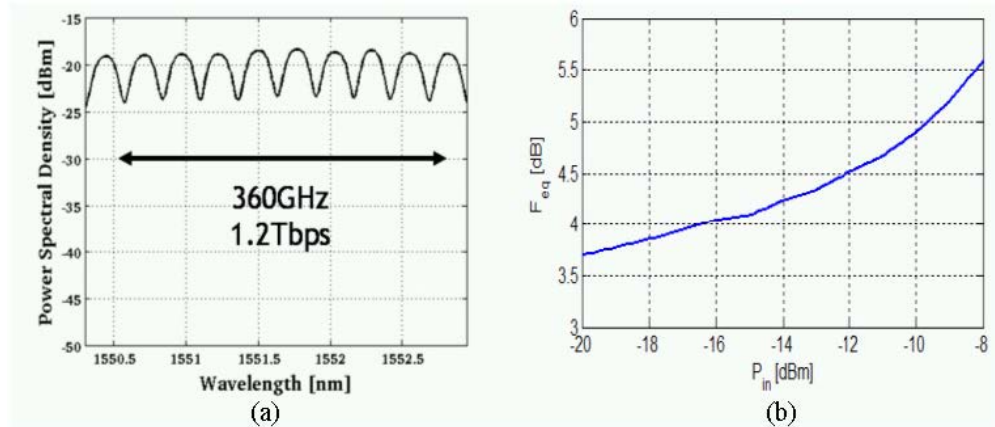


Fig. 2. (a) Spectrum of Tx WDM signal with ten PM-QPSK channels at 33GHz spacing (0.06 nm resolution). (b) Equivalent noise figure of the dual stage EDFA vs. total power at the input of the 1st stage EDFA.

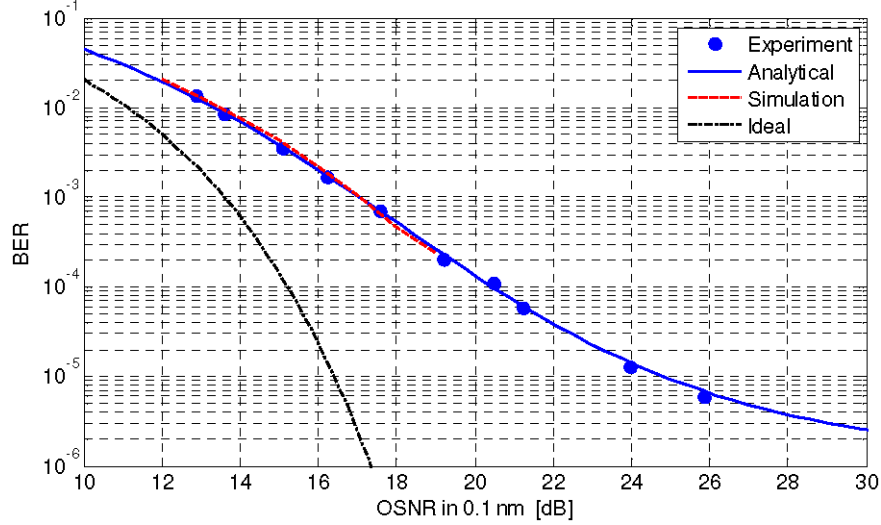


Fig. 3. Back-to-back performance of the system: matching of experimental results with analytical and simulative predictions. In this plot, being a back-to-back measurements, OSNR is due to ASE only.

interference (NLI), that we evaluate using Eq. (5) in [5] in case of spacing equal to the symbol-rate (Nyquist limit) or following the derivation presented in [11,12] for wider channel spacing.

In the absence of cross-talk or other transmitter impairments and assuming to operate with a receiver whose transfer function is matched to the transmitted pulses, the bit error rate (BER) for PM-QPSK modulation is given by [16]:

$$BER = \frac{1}{2} \operatorname{erfc} \left( \sqrt{OSNR_{NL} \frac{B_n}{2R_s}} \right) \quad (2)$$

where  $R_s$  is the baud-rate and  $OSNR_{NL}$  is the generalized OSNR that in case of back-to-back (btb) measurements is due to ASE noise only. The matched filter hypothesis is typically well verified because the adaptive equalizer in the receiver tends to such a transfer function. However, actual systems suffer from various transmitter and receiver impairments that modify the BER vs.  $OSNR_{NL}$  dependence. In order to reach our final goal of validating the propagation model, we need to properly take into account all these impairments. They must be calibrated out with a back-to-back measurement, in order to isolate them from the non-linear propagation effects. Figure 3 shows the back-to-back performance in terms of BER measured on the 5th channel of the WDM comb as a function of the  $OSNR_{NL}$ : being in btb condition in this case OSNR is referred to ASE noise only.

The penalty found in the back-to-back performance with respect to the ideal curve (shown in Fig. 3 as a dash-dotted black line) can be ascribed to two different categories of impairments described in the following.

- 1) Non-perfect matching between receiver filtering and transmitted pulses, which induces a rigid translation of the BER vs.  $OSNR_{NL}$  curve: it can be modeled inserting a factor  $k$  in the BER formula:

$$BER = \frac{1}{2} \operatorname{erfc} \left( \sqrt{k \cdot OSNR_{NL} \frac{B_n}{2R_s}} \right). \quad (3)$$

- 2) Cross-talk between adjacent channels and/or electrical non-idealities at the transmitter, which are responsible for an error floor at high  $OSNR_{NL}$  values. It can be modeled as an additive noise term  $\eta_{XT} P_{Tx,ch}$  proportional to the signal power:

$$OSNR_{NL} = \frac{P_{Tx,ch}}{P_{ASE} + P_{NLI} + \eta_{XT} P_{Tx,ch}}. \quad (4)$$

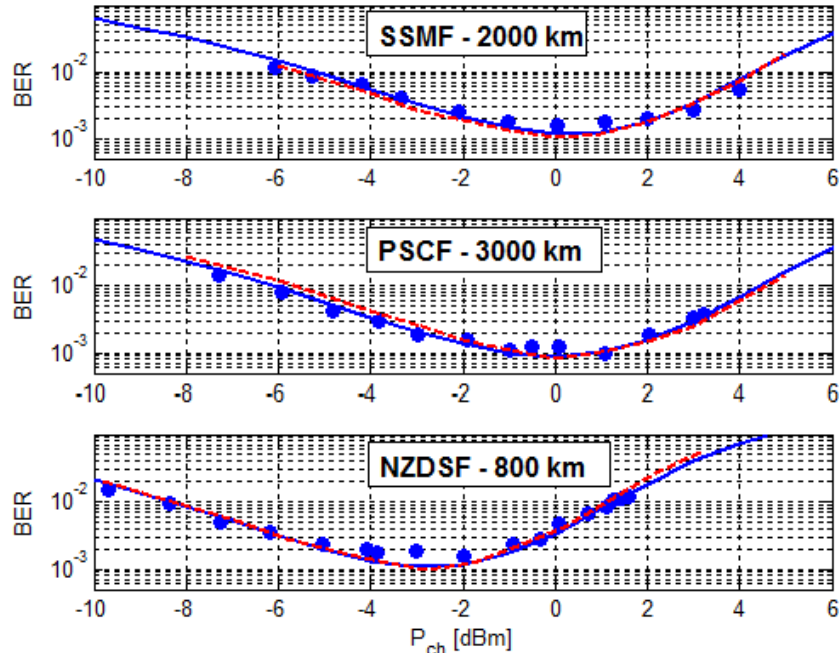


Fig. 4. Multi-span transmission experiment: comparison between experimental (blue dots), analytical (solid blue line) and simulative (dashed red line) results. BER vs. launch power per channel for SSMF, PSCF and NZDSF. System length changes with fiber type: see labels in each plot.

Both impairments were present in our experimental setup. For instance, due to the tight channel spacing used in the experiment ( $1.1 \cdot R_s$ ), a non-negligible amount of cross-talk from adjacent channels was impacting the performance in our setup. We therefore proceeded by best-fitting the values of  $k$  and  $\eta_{XT}$  in order to match the measured performance. The measured error floor in absence of optical noise (very high  $OSNR_{NL}$ ) was  $1.7 \cdot 10^{-6}$ . From this value we were able to calculate the value of  $\eta_{XT} = 0.045$ . Then, we determined the value of  $k$  best-fitting the whole BER curve, finding  $k = 1.26$ . Figure 3 shows an excellent agreement between the obtained analytical curve and the experiment values.

To further gain confidence with the model and in order to have another tool for evaluating the impact of fiber propagation and predict performances, we also set up a detailed simulative model of the system using the commercial system simulation tool OptSim<sup>TM</sup>. A careful modeling of each component allowed to take into account transmitter and receiver impairments together with channel crosstalk. We were able to reproduce the experimental btb curve with simulations as well. The number of simulated symbols was equal to  $2^{16}$ , thus the estimated BER values were reliable down to about  $BER = 2 \cdot 10^{-4}$  (which corresponds to  $\sim 50$  bit errors). Results presented in Fig. 3 show an excellent agreement between experiments and simulations.

#### 4. Transmission results

After back-to-back measurements for calibration of impairments and crosstalk, we carried out two sets of transmission experiments on a multi-span link mimicked with the recirculating loop described in Sec. 2. As our goal was the validation of the nonlinear model, we needed to minimize any other propagation impairments that could impact our signals. In particular Polarization dependent loss (PDL) was carefully kept under control. PDL in the loop was reduced by an optimized choice of in-loop devices and was constantly monitored from the Rx adaptive equalizer coefficients [17].

##### 4.1 Fixed distance measurements

We started out by measuring BER for the 5th channel in the WDM comb, at a fixed distance, sweeping the launched power per channel. The system length, given as number of recirculations, was chosen in order to obtain approximately the same minimum BER value, about  $10^{-3}$ , for all fibers: we selected 20, 30 and 8 recirculations for SSMF, PSCF and NZDSF, respectively. The fiber parameters used in both simulations and analytical calculations are those of Table 1. The span length was approximately 100 km in all cases.

Both in the analytical prediction and in simulation, the actual values of the EDFA equivalent noise figure, shown in Fig. 2(b) and varying with  $P_{in}$ , were taken into account together with calibrations presented in Sec. 3. In Fig. 4 we can observe an excellent agreement between experimental results (blue dots), analytical prediction (solid blue lines), and simulations (dashed red). Analytical predictions have been obtained using Eqs. (3) and (4), with  $P_{NLI}$  estimated by numerical integration of Eq. (4) in [5]. All predictions show almost coincident results, in particular the analytical model proved to be very accurate. As derived heuristically in [14],  $P_{NLI} = \eta_{NL} \cdot \gamma^2 \cdot N_{span} \cdot P_{Tx,ch}^3$  where  $N_{span}$  is the number of spans and the product  $(\eta_{NL} \cdot \gamma^2)$  is a “non-linear lever” that can be used to compare the strength of non-linear effects in different fiber types. In this paper we based the evaluation of  $P_{NLI}$  on the model presented in [5], that confirms the dependence on  $N_{span}$  and  $P_{Tx,ch}^3$ , and allows to analytically derive the entity of the “non-linear lever”  $(\eta_{NL} \cdot \gamma^2)$  in each different scenario. Values reported in Table 2 confirm the expected hierarchy among the three fibers under analysis and quantify the amount of non-linear effects. Note that the  $\eta_{NL}$  coefficient does not depend only on fiber parameters ( $\alpha$ ,  $D$  and  $\gamma$ ) but also on some relevant system parameters such as channel spacing ( $\Delta f$ ), symbol rate ( $R_s$ ) and number of channels ( $N_{ch}$ ). Values reported in Table 2 are valid for the specific system setup described in Section 2, but allow to compare the impact of non-linear effects in different fiber types when used in the same scenario.

##### 4.2 Maximum reach measurements

To further validate the model, we decided to carry out a second round of experiments. Here we targeted the evaluation of the maximum reach at the optimal launch power, for each of the three fiber types under analysis, given a target BER of  $10^{-3}$ . For each value of launch power per channel, we measured BER after each recirculation in order to assess the maximum number of spans the signal could propagate through while maintaining a BER below the target value. Figure 5 shows the maximum reachable distance as a function of launched power, for all three fibers under analysis: the y-axis is in logarithmic scale to obtain a straight line for the linear regime at low  $P_{Tx,ch}$ . Again, experimental results (blue dots) are in very good agreement with analytical predictions (solid blue lines) further validating the prediction

**Table 2. Fiber comparison through the “non-linear lever”**

	$\eta_{NL} \cdot \gamma^2$ [ $W^{-2}$ ]
SSMF	$8.10 \cdot 10^2$
PSCF	$5.13 \cdot 10^2$
NZDSF	$8.34 \cdot 10^3$

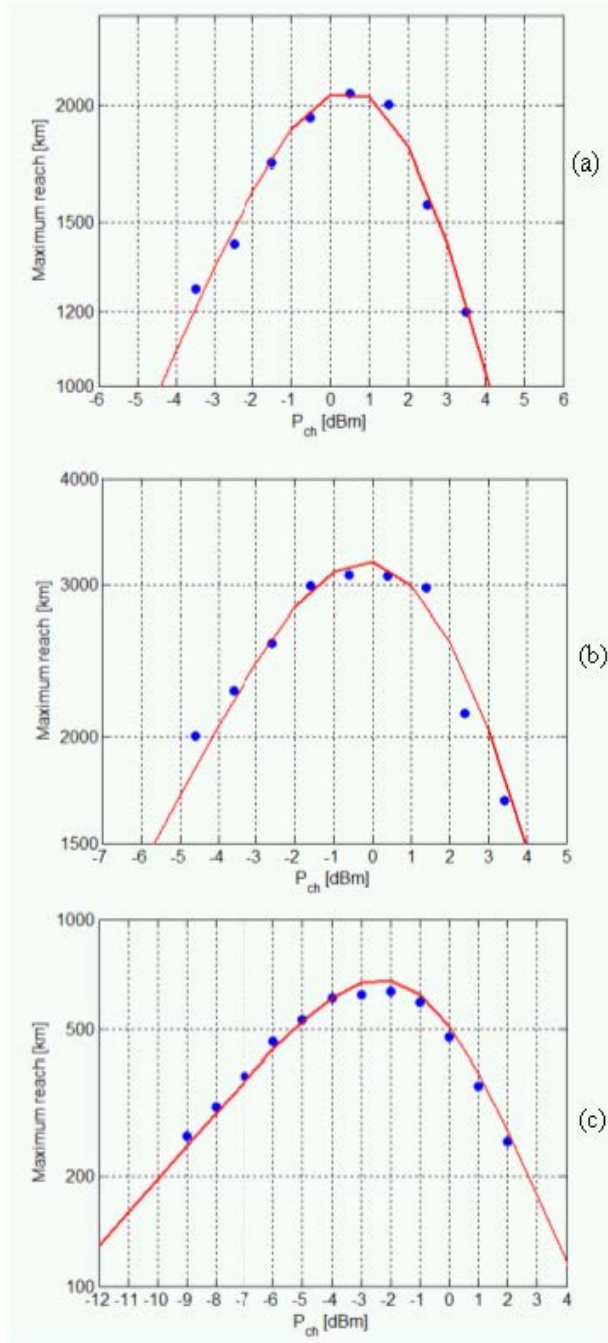


Fig. 5. Maximum reach measurements (blue dots) and analytical prediction (solid red line) for a target BER =  $10^{-3}$ : (a) SSMF, (b) PSCF and (c) NZDSF. Distances on the y-axis are presented in logarithmic scale.

capability of the model. In particular this second experiment shows that this nonlinear propagation model is reliable in predicting the optimal launch power, an important requirement for its possible application as a link design tool.



## 5. Conclusions

In conclusion, we have shown a comprehensive experimental validation of the non-linear propagation model described in [5] and [11,12] carried out over three fiber types with very different attenuation, dispersion and non-linearity parameters. We have first measured the BER dependence on launched power level and then the maximum reach at optimal launch power. In all cases considered, the model could predict experimental performance with a good level of accuracy. Simulations further confirmed the capability of the nonlinear propagation model of reliably predicting BER under all conditions.

In general, our results hint at the fact that most perturbative models which assume that non-linearity can be modeled as an additive Gaussian noise disturbance, such as [5–10], are accurate enough to successfully predict performance of system with coherent detection when propagating in uncompensated links. This class of models stands as a promising solution for the analysis of nonlinear propagation to be employed in future link design tools.

## Acknowledgments

We thank Sumitomo Electric Industries for providing the Z-plus PSCF fiber. The simulator OptSim<sup>TM</sup> was supplied by RSoft Design Group Inc. This work was supported by CISCO Systems (SRA contract) and by the EURO-FOS Network of Excellence funded by the European Commission in the 7th ICT-Framework Programme.